A&A 664, L1 (2022)
https://doi.org/10.1051/0004-6361/202243961

Astronomy & Astrophysics

LETTER TO THE EDITOR

Backtracing the internal rotation history of the β Cep star HD 129929

S. J. A. J. Salmon, F. D. Moyano, P. Eggenberger, L. Haemmerlé, and G. Buldgen

Observatoire de Genève, Université de Genève, Ch. Pegasi 51, 1290 Sauverny, Switzerland
e-mail: sebastien.salmon@unige.ch

Received 5 May 2022 / Accepted 19 July 2022

ABSTRACT

Context. HD 129929 is a slowly rotating β Cephei pulsator with a rich spectrum of detected oscillations, including two rotational multiplets. The asteroseismic interpretation revealed the presence of radial differential rotation in this massive star of ~9.35 $M_\odot$. The stellar core is indeed estimated to spin ~3.6 times faster than the surface. The surface rotation was consequently derived as $v \sim 2\,\mathrm{km\,s^{-1}}$. This massive star represents an ideal counterpart to the wealth of space-based photometry results for main-sequence and evolved low-mass stars. Those latter stars have revealed a new, and often unexpected, picture of the angular momentum transport processes acting in stellar interiors.
Aims. We investigate in a new way the constraints on the internal rotation of HD 129929, as a marker of the evolution of the internal rotation during the main sequence of a massive star. We test both hydrodynamic and magnetic instability transport processes of angular momentum.
Methods. We used the best asteroseismic model obtained in an earlier work. We calibrated stellar models including rotation, with different transport processes, to reproduce that reference model. We then looked to determine whether one process is favoured to reproduce the rotation profile of HD 129929, based on the fit of the asteroseismic multiplets.
Results. The impact of the Tayler magnetic instability on the angular momentum transport predicts a ratio of the core-to-surface rotation rate of only 1.6, while the recently revised prescription of this mechanism predicts solid-body rotation. Both are too low in comparison with the asteroseismic inference. The models with only hydrodynamic processes are in good agreement with the asteroseismic measurements. Strikingly, we can also get a constraint on the profile of rotation on the zero age main sequence: likely, the ratio between the core and surface rotation was at least ~1.7.
Conclusions. Transport of angular momentum by the Tayler magnetic instability is discarded for this star. The models with pure hydrodynamical processes reproduce the asteroseismic constraints. This result is specific to a slow rotator and has to be verified more generally in other massive main-sequence stars. Constraints on the rotation in earlier stages of this star also offer a new opportunity to test the impact of accretion during the pre-main sequence evolution.

Key words. asteroseismology – stars: early-type – stars: rotation – stars: individual: HD 129929

1. Introduction

We have witnessed a leap in our knowledge of the internal rotation in intermediate- and low-mass stars thanks to space-based asteroseismology. At first, the determination of the core rotation rate in a large sample of red giants (Mosser et al. 2012; Gehan et al. 2018) or precise radial profiles in subgiants and red giants (e.g., Beck et al. 2012; Deheuvels et al. 2012, 2014, 2015; Triana et al. 2017; Di Mauro et al. 2018; Fellay et al. 2021) has revealed values in strong disagreement with theoretical model predictions. It has pinpointed the need for (an) additional mechanism(s) to extract angular momentum (AM) out of the core layers efficiently (e.g., Eggenberger et al. 2012, 2017, 2019b; Ceillier et al. 2013; Marques et al. 2013; Deheuvels et al. 2020). We also had access to the rotation rates in the vicinity of the core layers of hundreds of γ Dor pulsators (e.g., Van Reeth et al. 2016; Ouazzani et al. 2017; Zwintz et al. 2017; Christophe et al. 2018; Li et al. 2019, 2020), which are main-sequence progenitors of red giants. For a reduced sample of them, the rotation contrast between the core and envelope or surface was obtained, revealing almost rigid profiles of rotation (e.g., Kurtz et al. 2014; Saio et al. 2015; Murphy et al. 2016; Li et al. 2019, 2020; Saio et al. 2021). The preliminary work by Ouazzani et al. (2019) on these results also hints at the need for an additional transport process of AM during the main sequence. With results from other types of stars, we are starting to have a view of the AM transport processes needed all across the Hertzsprung–Russell (HR) diagram (see review by Aerts et al. 2019).

The β Cephei pulsators are natural candidates for exploring transport mechanisms in more massive cases (e.g., Bowman 2020; Salmon et al. 2022). These main-sequence stars between ~8 and 25 $M_\odot$ present mixed-modes of oscillation probing the layers at the boundary of the stellar core, as well as pressure modes sounding the radiative envelope. They were among the first for which asteroseismology measured rotation rates in the stellar core and surface (as of today, in five pulsators: Aerts et al. 2003; Briquet et al. 2007; Dziembowski & Pamyatnykh 2008; Desmet et al. 2009; Burssens et al. 2021). Too few or putative rotationally associated non-axisymmetric modes were also reported in other β Cep stars (e.g., Mazumdar et al. 2006; Aerts et al. 2006; Briquet et al. 2009; Handler et al. 2009;

Aerts et al. 2011; Briquet et al. 2012), which nevertheless makes them promising targets to increase the sample with known internal rotation. In the confirmed cases, except for θ Oph, a clear indication of radial differential rotation was found for the other four pulsators, with core-to-surface ratios Ω_c/Ω_S between ~2 and ~8.

In an attempt to contextualise these measurements, Suárez et al. (2009) showed, in the case of ν Eri, that between the two extreme hypotheses of rigid rotation and the local conservation of AM, the latter was preferred to reproduce the asteroseismic data. We here focus on HD 129929, for which the implication of different AM transport processes was not investigated. Formally confirmed as a β Cep star by Waelkens & Rufener (1983), a dedicated campaign of observation (Aerts et al. 2004, hereafter A04) led to the detection of frequency members of two multiplets, which offered the opportunity to probe the internal rotation (Aerts et al. 2003). A detailed asteroseismic modelling of this star was carried out by Dupret et al. (2004, hereafter D04), who derived a core-to-surface rotation ratio of ~3.6, assuming a radial linear decrease in the rotation rate in the stellar interior.

We have extended the analysis of D04, by focussing on the question of the internal rotation and its evolution during the main sequence in HD 129929. We used Geneva models including detailed treatment of rotation by hydrodynamic and magnetic instabilities to determine which transport mechanisms lead to profiles of rotation in accordance with the one calibrated from asteroseismology.

We start by recalling, in Sect. 2, the properties of HD 129929 and presenting the physics of the different stellar models used in our analysis. In Sect. 3 we show how the seismic constraints mark out the rotational profile of the star and its past evolution. In Sect. 4, we discuss the implications of the determined rotation profile for different AM transport processes, before concluding.

2. Dataset and methods

We report, in Table 1, the observational frequency dataset determined by A04, and based on it, the properties of the best-fitting model found by D04. This asteroseismic modelling unambiguously identified the frequencies (ν) as those of the radial fundamental pressure mode p_1[1]; the complete p_1, ℓ_1 mode triplet; and two consecutive azimuthal-order components of the g_1, ℓ_2 quintuplet. The frequency shifts between different azimuthal orders in multiplets depend on the rotation rate in specific regions of the star (see Sect. 2.2). The triplet shows a small asymmetry, and we use its averaged splitting value (as in D04), $\Delta_{p_1} = 0.012130$ c/d. The other splitting is $\Delta_{g_1} = 0.012109$ c/d. The observational accuracy error on the frequencies was estimated to $\sim 10^{-6}$ c/d.

2.1. Stellar models

We did not perform a new asteroseismic modelling of the star since the results by D04 adequately reproduced the observed frequencies. We thus adopted the properties of their best stellar model. The best-fit asteroseismic model found by the authors revealed that HD 129929 is most likely a ~9.35 $M_\odot$ star in the middle of its main-sequence hydrogen-burning phase. We adopted those stellar parameters (see Table 1) to recompute a representative stellar model of HD 129929. This was done with the same stellar evolution code, CLES (Scuflaire et al. 2008b),

[1] We use p_i or g_i to designate the ith radial order of a pressure or gravity mode, respectively, while ℓ_i stands for the angular degree i.

Table 1. Mode frequencies detected in HD 129929 (from A04) and parameters of the best stellar model reproducing this dataset (from D04).

Seismic frequencies [c/d]	Asteroseismic model
$\nu\,(p_1, \ell_0) = 6.590940$	$M = 9.35\,M_\odot$; $\log g = 3.905$
$\nu\,(p_1, \ell_1) = 6.966172$–$6.978305$–	$T_{\rm eff} = 22\,392$ K; $X_c = 0.353$
6.990431	$X_i = 0.7$; $Z_i = 0.0188$
$\nu\,(g_1, \ell_2) = 6.449590$–$6.461699$	$\alpha_{ov} = 0.1$

Notes. $T_{\rm eff}$ is the effective temperature; $\log g$ the surface gravity; X_c, the central H abundance; X_i and Z_i the initial H and metal mass fractions; and α_{ov} the overshooting parameter.

and following the same input physics as in D04 (see details in their paper). We assumed full redistribution or local conservation of AM, and verified whether they could predict an internal rotation profile reproducing the rotational splittings of the observed frequencies.

In a second step, we aimed to interpret the asteroseismic constraints on the rotation profile in terms of AM transport mechanisms possibly at work in massive stars. We hence computed models including a coherent treatment of the rotation, with the mean of the Geneva stellar evolution code (GENEC, Eggenberger et al. 2008). The code relies on the assumption of shellular rotation as developed in Zahn (1992). It takes into account the meridional currents and shear instability for the estimation of AM transport along the evolution of the stellar models. It can also account for the impact of magnetic instabilities, following the Tayler–Spruit dynamo (Spruit 2002), or its revision proposed by Fuller et al. (2019). The advecto-diffusive equation for the transport of AM in (a) radiative zone(s) while accounting for the aforementioned processes reads as follows:

$$\rho \frac{\mathrm{d}}{\mathrm{d}t}(r^2\Omega) = \frac{1}{5r^2}\frac{\partial}{\partial r}(\rho r^4 \Omega U) + \frac{1}{r^2}\frac{\partial}{\partial r}\left[(D_{\rm shear} + \nu_{\rm M})\rho r^4 \frac{\partial \Omega}{\partial r}\right], \quad (1)$$

where r is the radius, and ρ and Ω are the mean density and mean angular velocity on an isobar, respectively. The radial component of the meridional circulation is given by U. The diffusion coefficient $D_{\rm shear}$ is the one for the transport of AM by the shear instability (following Maeder 1997), while $\nu_{\rm M}$ represents the diffusion coefficient from magnetic instabilities. When no magnetic instability is considered, $\nu_{\rm M} = 0$ and the models then computed are referred to as pure hydrodynamical. The magnetic instabilities accounting for the transport of AM were computed first following the original prescription of the Tayler–Spruit dynamo. In this case, $\nu_{\rm M}$ takes the form of the $\nu_{\rm TS}$ coefficient as given in Eggenberger et al. (2019a, see their Eqs. (1)–(2)). As recalled by these authors, to whom we refer interested readers for details, this mechanism works in regions presenting shear and is activated above a triggering threshold, but it is inhibited by chemical gradients. We also considered the Fuller revision of this mechanism, in which case $\nu_{\rm M}$ takes the form of $\nu_{\rm T}$ as given in Eq. (3) of Eggenberger et al. (2019a). These Geneva models were constructed to reproduce the stellar properties of the asteroseismic model as recalled in Table 1.

2.2. Rotational splittings

The frequency separation of different azimuthal-order modes in a multiplet is directly related to the rotation rate in the layers where these modes propagate. For stars with rotation frequencies much

smaller than the oscillation frequencies, a simple perturbation approach can be used. We only considered a first-order expression since HD 129929 is a clear slow rotator, $v \sin i \lesssim 13\,\mathrm{km\,s^{-1}}$: in comparison, stars with similar spectral types present projected velocities between 160 and 200 $\mathrm{km\,s^{-1}}$ on average (e.g., Royer 2009). The first order only accounts for Coriolis effects, while higher-order terms also account for centrifugal effects (see e.g., Goupil 2011). As mentioned earlier, here the Δ_{p_1} splitting presents a small asymmetry ($\sim 7 \times 10^{-6}$ c/d). Although such a feature is expected from higher-order effects of rotation, the rotation velocity of the star is so low that these effects are likely to be negligible. This is in line with computations up to the third order for a typical β Cep model at various rotation rates presented in Ouazzani & Goupil (2012). Limiting to the first order, as demonstrated by Ledoux (1951), the shift in the frequency of a non-axisymmetric mode then reads as follows:

$$\nu_{n,\ell,m} = \nu_{n,\ell,0} + m \int_0^R K_{n,\ell} \Omega \, \mathrm{d}r, \tag{2}$$

where ν is the frequency of a (n, ℓ, m) mode, n the radial order, m the azimuthal order, R the stellar radius, and $K_{n,\ell}$ the rotational kernel of the mode. The latter is built from the mode eigenfunctions and has to be computed from a stellar structure model. Hence, it must be representative of the star under investigation. This is why we recomputed the asteroseismic solution of D04; from this stellar model, we derived the rotational kernels of the p_1,ℓ_1 and g_1,ℓ_2 modes with the LOSC adiabatic oscillation code in its standard setting (see details in Scuflaire et al. 2008a).

We finally tested the ability of various rotation profiles $\Omega(r)$ to reproduce the observed values of Δ_{p_1} and Δ_{g_1} by comparing the theoretical counterparts of these splittings, evaluated with Eq. (2), and using the following simple merit function:

$$\chi^2 = \frac{1}{2} \sum_{i=1}^{2} \frac{(\Delta_{\mathrm{obs,i}} - \Delta_{\mathrm{th},i})^2}{\sigma_i^2}, \tag{3}$$

with σ_i^2 being the observational error (σ_i is set to 10^{-6} c/d).

3. Analysis of the internal rotation constraints

We show in Fig. 1, as dotted lines, the kernels $K_{1,1}$ and $K_{-1,2}$ associated with the observed splittings Δ_{p_1} and Δ_{g_1}, respectively. Once computed the integrals of the former, it is straightforward that the splittings cannot be reproduced with a rigid rotation profile, as stated previously in Aerts et al. (2003). This discards the assumption of full redistribution of AM in the star during its evolution.

We then assumed the opposite with no redistribution of AM by including local conservation alongside the stellar evolution. We first considered a case where a rigid profile is assumed on the zero age main sequence (ZAMS). We found that once evolved to the current stage of HD 129299, the minimum value in χ^2 is very large, 2.64×10^5, as depicted in the right panel of Fig. 2. The rotation profiles corresponding to this solution are shown in green in Fig. 1, both at the ZAMS and once at the current age of HD 129929. We notice very small wiggles (as well for the blue curve) of the profile in the envelope, which here result from the number of points describing the model and the numerical integration scheme used to follow the AM conservation along the stellar track, without an impact on the computed splittings. As indicated by the large χ^2 value, the ratio between the core and surface rotation rates of this green profile is too small and cannot reproduce the splittings. In the right insert of this figure, we

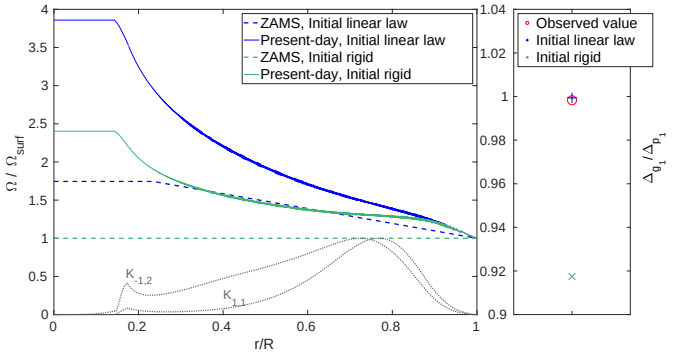

Fig. 1. Normalised profiles of rotation in the CLES model of HD 129929 (solid lines) as a function of the normalised radius. The profiles are those that best fit the observed rotational splittings, assuming a rigid (green) or linear (blue) law on the ZAMS and local AM conservation during evolution. The related ZAMS profiles (corresponding to the minimums in χ^2 shown in Fig. 2) are shown with dashed lines. The normalised rotational kernels of the p_1 and g_1 modes are represented by the grey dotted lines. The right insert shows a comparison of the splitting ratio between the observed value (red) and these best-fit solutions assuming a rigid (blue) or linear (green) profile of rotation on the ZAMS.

provide the ratio of the splittings ($\Delta_{g_1}/\Delta_{p_1}$), which here is an estimate of the rotation contrast between the core and envelope. The splitting ratio of this model with a rigid rotation on the ZAMS is clearly lower than the observed value, confirming it has a rotation contrast that is too low between its core and surface.

However, during their early stages of evolution, stars of $\sim 9\,M_\odot$ are fully radiative during a large fraction of the accretion phase (Haemmerlé et al. 2019). Once the star reaches the ZAMS, most of the radiative layers are radiative since they were accreted, avoiding convective AM transport. In these short timescales of the pre-main sequence phase (a few 10^5 yr for a $9\,M_\odot$), meridional circulation and shear diffusion are expected to remain negligible, in particular for slow rotators, so that each radiative layer keeps the AM it advected at accretion as the star contracts, and the rotation profile essentially reflects the AM accretion history (Haemmerlé et al. 2017) given by the rotational properties of the pre-stellar cloud. We thus assumed a non-rigid profile on the ZAMS, with rigid rotation in the convective core, and a simple linear relation in the radiative envelope. Letting the model evolve at the age of HD 129929, we succeeded at finding a rotation profile that reproduces the splittings. The solution is well defined and non-degenerate, as shown in the left panel of Fig. 2. Starting with an initial[2] $\Omega_{\mathrm{ZAMS,C}}/\Omega_{\mathrm{ZAMS,S}}$ of 1.74, the profile evolves to a present-day value of 3.86. In the right insert of Fig. 1, this model reproduces the observed splitting ratio, confirming that its profile of rotation (blue line in the left panel) presents an adequate contrast between the core and surface. This is in good agreement with the simpler linear model of D04, which revealed a similar contrast between the core and surface. The freedom of varying the rotation profile to reproduce the splittings is actually limited in this case as a result of the two kernels we have at our disposal. More specifically, $K_{-1,2}$ (see Fig. 1) is clearly associated with a mixed mode. While it bears all the information we have on the central layers, it nevertheless is sensitive to a large extent to the envelope and surface layers, due to its larger amplitude in these regions.

[2] $\Omega_{\mathrm{ZAMS,C}}$ and $\Omega_{\mathrm{ZAMS,S}}$ are the core and surface rotation rates at the ZAMS, respectively.

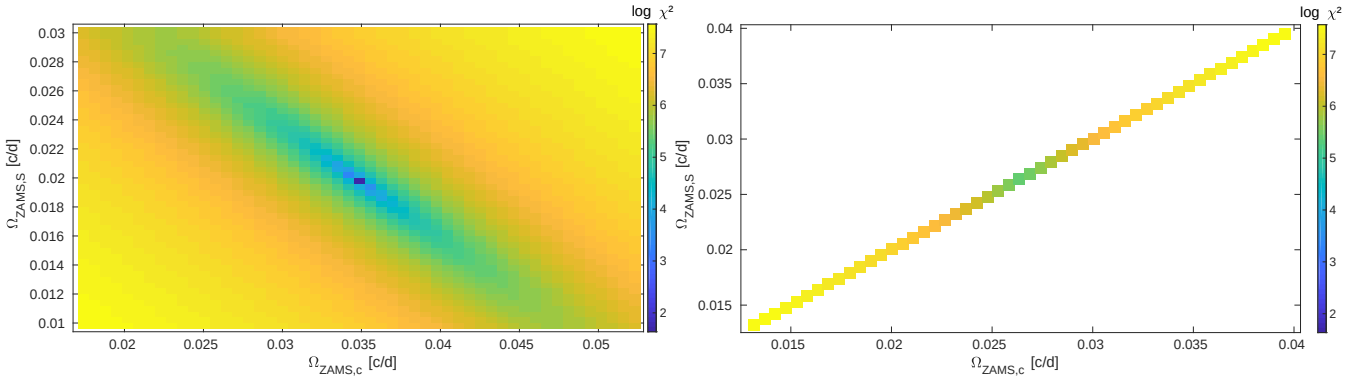

Fig. 2. Map of the χ^2 values based on the comparison of HD 129929 observed and theoretical rotational splittings, as in Eq. (3), assuming a linear (*left panel*) or rigid (*right panel*) profile of rotation on the ZAMS, and local AM conservation along the evolution to the current stage of the star.

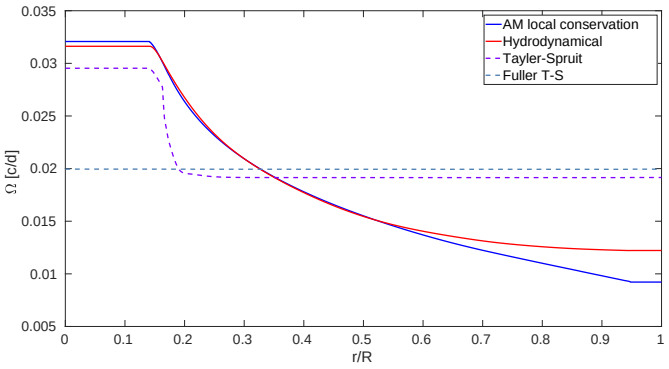

Fig. 3. Profiles of rotation as a function of the normalised radius for the different Geneva models of HD 129929. The different mechanisms of AM transport included in each model are indicated in the legend. Dotted lines distinguish the cases that include magnetic instabilities.

4. Angular momentum transport processes

Assuming local AM conservation throughout the MS evolution yields a realistic profile of rotation that is able to reproduce the observational splittings, but also unambiguously gives a picture of it at the ZAMS. We thus compared this solution to more sophisticated stellar models that treat AM transport with physically motivated mechanisms. This was done with 9.35 $M_\odot$ Geneva models as explained in Sect. 2.1. The linear rotation profile on the ZAMS that we determined in Sect. 3 was adopted as an initial condition for these refined models. The models were calibrated to reproduce the same location in the HR diagram as the CLES model of HD 129929. We compared their structure and found that the quantities relevant for asteroseismic properties were very similar between CLES and GENEC models.

The profiles of rotation resulting from the different transport mechanisms used through the evolution of the models are shown in Fig. 3. The hydrodynamical model predicts a very similar profile as in the local conservation assumption. Meridional circulation is the main driver of AM transport through advection at large scales. However, in the present case, we dealt with a slow rotator, and the circulation is consequently very weak, resulting in a limited transport of AM. Since the hydrodynamical model is very close to the one with AM local conservation, the profile of rotation that it predicts is in accordance with the asteroseismic constraints for this star.

We also show the two profiles of rotation obtained with the magnetic instabilities, either following the original prescription of the Tayler–Spruit dynamo or the Fuller revision. In the former case, differential rotation can, however, develop close to the convective core where the chemical gradient weakens the instability, allowing for an efficient transport of AM later on. Yet, the contrast between the centre and surface cannot account for the asteroseismic constraints. Furthermore, the contrast developed by this mechanism is relatively insensitive to the initial conditions. In the latter case, the AM transport is much more efficient and leads to rigid rotation, which is clearly discarded in this star. The coupling between central and superficial layers in these two models with magnetic instabilities are both too strong: thus, the asteroseismic observations in the case of the HD 129929 star do not favour such instabilities.

5. Conclusion

Starting from the well-established asteroseismic solution for the β Cep star HD 129929, we have studied, in detail, the consequences of its asteroseismic properties on the internal rotation of the star, including its past evolution on the main sequence. Assuming local conservation of angular momentum during the main sequence, we have determined a non-degenerate solution showing that the present-day rotation at the centre of the star is probably ∼3.86 times greater than at the surface. This result is in good agreement with the solution found by D04, which was a factor of 3.6. The latter relies on the approximation of a linear decreasing law of the rotation rate from the convective core to the surface, without consideration for the past evolution of the star.

Given the non-degeneracy of the solution obtained under local conservation of angular momentum, we could backtrace the evolution of the internal rotation of this star. Assuming a linear law for the profile of rotation on the ZAMS, we have determined that the core of the star was at that time rotating at least ∼1.74 times faster than the surface. This result highlights the potential for asteroseismology not only to constrain the current structure of a massive star, but also conditions prevailing in its early stages of evolution. The limits given on the internal rotation at the ZAMS are offering a new testbed for conditions of formation of these stars and their pre main-sequence evolution, and for example, how angular momentum redistributes during episodes of accretion (Haemmerlé et al. 2017).

In a subsequent step, we have compared our asteroseismic solution to the rotational profiles predicted by models representative of HD 129929, including different transport processes. First considering the sole combination of meridional circulation and shear instability, we found it leads to a very low degree of

redistribution of the angular momentum: the meridional circulation is hindered to act efficiently because the star is a slow rotator (our asteroseismic solution predicts a surface velocity of $2.29\,\mathrm{km\,s^{-1}}$). It leads to a core-to-surface ratio fully compatible with the asteroseismic profile deduced in the star. Models which included magnetic instabilities, either the Tayler–Spruit dynamo or its Fuller revision, show a strong coupling between the core and envelope. As a result, there is an efficient redistribution of angular momentum that flattens the profiles of rotation, which is clearly rejected by the asteroseismic constraints in this case.

While magnetic instabilities are good candidates for explaining the profile of rotation in the Sun (Eggenberger et al. 2019a) or partially low-mass stars in evolved stages (e.g., Fuller et al. 2019), HD 129929 is a first proven example of their inadequacy in a main-sequence massive star. To the contrary, the pure hydrodynamical case appears to be a good candidate to explain the rotational properties of this star. This is in contrast to the conclusions for low- and intermediate-mass stars, in which additional transport processes are expected (e.g., Ouazzani et al. 2019; Eggenberger et al. 2019b). The present case remains particuliar as HD 129929 is a slow rotator. Following our effort, the other β Cep stars for which we have rotational splittings will allow us to further constrain the transport processes at work in massive stars.

Acknowledgements. We are grateful to G. Meynet and M.-A. Dupret for helpful discussions and remarks on this work. S.J.A.J.S., F.D.M., P.E. and L.H. have received funding from the European Research Council (ERC) under the European Union's Horizon 2020 research and innovation program (grant agreement No 833925, project STAREX). G.B. acknowledges funding from the SNF AMBIZIONE grant No. 185805 (Seismic inversions and modelling of transport processes in stars).

References

Aerts, C., Thoul, A., Daszyńska, J., et al. 2003, Science, 300, 1926
Aerts, C., Waelkens, C., Daszyńska-Daszkiewicz, J., et al. 2004, A&A, 415, 241
Aerts, C., Marchenko, S. V., Matthews, J. M., et al. 2006, ApJ, 642, 470
Aerts, C., Briquet, M., Degroote, P., Thoul, A., & van Hoolst, T. 2011, A&A, 534, A98
Aerts, C., Mathis, S., & Rogers, T. M. 2019, ARA&A, 57, 35
Beck, P. G., Montalban, J., Kallinger, T., et al. 2012, Nature, 481, 55
Bowman, D. M. 2020, Front. Astron. Space Sci., 7, 70
Briquet, M., Morel, T., Thoul, A., et al. 2007, MNRAS, 381, 1482
Briquet, M., Uytterhoeven, K., Morel, T., et al. 2009, A&A, 506, 269
Briquet, M., Neiner, C., Aerts, C., et al. 2012, MNRAS, 427, 483
Burssens, S., Bowman, D. M., Michielsen, M., Simón-Díaz, S., & Aerts, C. 2021, Posters from the TESS Science Conference II (TSC2), 75
Ceillier, T., Eggenberger, P., García, R. A., & Mathis, S. 2013, A&A, 555, A54
Christophe, S., Ballot, J., Ouazzani, R. M., Antoci, V., & Salmon, S. J. A. J. 2018, A&A, 618, A47
Deheuvels, S., García, R. A., Chaplin, W. J., et al. 2012, ApJ, 756, 19
Deheuvels, S., Doğan, G., Goupil, M. J., et al. 2014, A&A, 564, A27
Deheuvels, S., Ballot, J., Beck, P. G., et al. 2015, A&A, 580, A96
Deheuvels, S., Ballot, J., Eggenberger, P., et al. 2020, A&A, 641, A117
Desmet, M., Briquet, M., Thoul, A., et al. 2009, MNRAS, 396, 1460
Di Mauro, M. P., Ventura, R., Corsaro, E., & Lustosa De Moura, B. 2018, ApJ, 862, 9
Dupret, M.-A., Thoul, A., Scuflaire, R., et al. 2004, A&A, 415, 251
Dziembowski, W. A., & Pamyatnykh, A. A. 2008, MNRAS, 385, 2061
Eggenberger, P., Meynet, G., Maeder, A., et al. 2008, Ap&SS, 316, 43
Eggenberger, P., Montalbán, J., & Miglio, A. 2012, A&A, 544, L4
Eggenberger, P., Lagarde, N., Miglio, A., et al. 2017, A&A, 599, A18
Eggenberger, P., Buldgen, G., & Salmon, S. J. A. J. 2019a, A&A, 626, L1
Eggenberger, P., Deheuvels, S., Miglio, A., et al. 2019b, A&A, 621, A66
Fellay, L., Buldgen, G., Eggenberger, P., et al. 2021, A&A, 654, A133
Fuller, J., Piro, A. L., & Jermyn, A. S. 2019, MNRAS, 485, 3661
Gehan, C., Mosser, B., Michel, E., Samadi, R., & Kallinger, T. 2018, A&A, 616, A24
Goupil, M. 2011, in Lecture Notes in Physics, eds, J. P. Rozelot, & C. Neiner (Berlin: Springer Verlag), 832, 223
Haemmerlé, L., Eggenberger, P., Meynet, G., et al. 2017, A&A, 602, A17
Haemmerlé, L., Eggenberger, P., Ekström, S., et al. 2019, A&A, 624, A137
Handler, G., Matthews, J. M., Eaton, J. A., et al. 2009, ApJ, 698, L56
Kurtz, D. W., Saio, H., Takata, M., et al. 2014, MNRAS, 444, 102
Ledoux, P. 1951, ApJ, 114, 373
Li, G., Van Reeth, T., Bedding, T. R., Murphy, S. J., & Antoci, V. 2019, MNRAS, 487, 782
Li, G., Van Reeth, T., Bedding, T. R., et al. 2020, MNRAS, 491, 3586
Maeder, A. 1997, A&A, 321, 134
Marques, J. P., Goupil, M. J., Lebreton, Y., et al. 2013, A&A, 549, A74
Mazumdar, A., Briquet, M., Desmet, M., & Aerts, C. 2006, A&A, 459, 589
Mosser, B., Goupil, M. J., Belkacem, K., et al. 2012, A&A, 548, A10
Murphy, S. J., Fossati, L., Bedding, T. R., et al. 2016, MNRAS, 459, 1201
Ouazzani, R. M., & Goupil, M. J. 2012, A&A, 542, A99
Ouazzani, R.-M., Salmon, S. J. A. J., Antoci, V., et al. 2017, MNRAS, 465, 2294
Ouazzani, R. M., Marques, J. P., Goupil, M. J., et al. 2019, A&A, 626, A121
Royer, F. 2009, The Rotation of Sun and Stars, 765, 207
Saio, H., Kurtz, D. W., Takata, M., et al. 2015, MNRAS, 447, 3264
Saio, H., Takata, M., Lee, U., Li, G., & Van Reeth, T. 2021, MNRAS, 502, 5856
Salmon, S. J. A. J., Eggenberger, P., Montalbán, J., et al. 2022, A&A, 659, A142
Scuflaire, R., Montalbán, J., Théado, S., et al. 2008a, Ap&SS, 316, 149
Scuflaire, R., Théado, S., Montalbán, J., et al. 2008b, Ap&SS, 316, 83
Spruit, H. C. 2002, A&A, 381, 923
Suárez, J. C., Moya, A., Amado, P. J., et al. 2009, ApJ, 690, 1401
Triana, S. A., Corsaro, E., De Ridder, J., et al. 2017, A&A, 602, A62
Van Reeth, T., Tkachenko, A., & Aerts, C. 2016, A&A, 593, A120
Waelkens, C., & Rufener, F. 1983, A&A, 119, 279
Zahn, J.-P. 1992, A&A, 265, 115
Zwintz, K., Van Reeth, T., Tkachenko, A., et al. 2017, A&A, 608, A103